Supporting Information

UV-modification of Ag nanoparticles on α-MoC_x for interfaces polarization engineering in electromagnetic wave absorption

Pengyuan Zhu[a]†, Yifan Kang[a]†*, Xinglong Li[b] Haoquan Yu[b], Tong Liu[a,d], Ming Song[a], Yanan Zhang[a], Lifan Zhou[c]*, Ping Zhao[b]*, and Wenhuan Huang[a]*

a Key Laboratory of Chemical Additives for China National Light Industry, College of Chemistry and Chemical Engineering, Shaanxi University of Science and Technology, Xi'an 710021, P. R. China.

b School of Chemistry and Chemical Engineering, Guangdong Pharmaceutical University, Education Mega Centre, No. 280, Wai Huan Dong Road, Guangzhou 510006, PR. China.

c Shaanxi Electronic Information Research Institute Co. Ltd., Xian 710061, P. R. China.

d College of New Energy, Xi'an Shiyou University, Xi'an 710065, China.

† These authors contribute equally to this work

1. Experimental Section

1.1. Synthesis of α-MoC polyhedrons

In the synthesis of α-MoC, the 5.3 g (24.2 mmol) of Zn $(OAc)_2$•$2H_2O$, 2.88 g (35.1 mmol) of 2-methylimidazole, 0.75 g H_2MoO_4 (4.63 mmol) were soluble in 100 mL DMF and kept stirring at 160 °C for 96 h. After the mixture was cooled down to ambient temperature naturally, the HZIF-ZnMo powder was obtained. The white powder was then centrifugal collected, ethanol washed and dried at room temperature. Finally, the black α-MoC was obtained by calcining in a nitrogen stream at 800°C for 2 h.

1.2. Synthesis of α-Mo@Ag polyhedrons

In the synthesis of α-MoC@Ag, 1 mL of $AgNO_3$ solution (10 mmol/L) was dispersed dropwise into 2 mL (1 mg/mL) of α-MoC solution under ultrasonication. Under stirring, the above mixed solution was illuminated with a UV lamp (365 nm, 50 W) for different durations of 0.5, 1.0, 1.5, and 2.0 h. After the UV treatment, the precipitate was obtained by centrifugation and cleaned several times with deionized water to extract the unreacted $AgNO_3$. The α-MoC@Ag polyhedrons were thus obtained as the outgrowth. α-MoC@Ag irradiated for 0.5, 1.0, 1.5, and 2.0 h were named as α-MoC@Ag-0.5, α-MoC@Ag-1.0, α-MoC@Ag-1.5 and α-MoC@Ag-2.0 respectively. The polyhedron without UV irradiation was named as α-MoC.

2. Characterizations

D8 DAVANCI X-ray powder diffractometer equipped with graphite monochromatized Cu Kα radiation (λ = 0.1542 nm) was used to record powder X-ray diffraction (PXRD) patterns in the 2θ range of 5°-80° with a scanning rate of 1 °/min. Scanning electron microscopy (SEM) images were collected by a Hitachi S4800 apparatus with an acceleration voltage of 2 kV. The transmission

electron microscopy (TEM) images were recorded on a JEM-2010HR apparatus working at an accelerating voltage of 200 kV and X-ray energy-dispersive spectroscopy (EDS) was taken on a JEM-2010HR-Vantage typed energy spectrometer. X-ray photoelectron spectroscopy (XPS) was implemented on Thermo ESCA Lab250XI. Raman spectroscopy of the samples was obtained by a Renishaw in Via Raman Microscope. The electromagnetic parameters were analyzed using a HP8753D vector network analyzer in the frequency range of 2-18 GHz. The measured samples were dispersed in paraffin homogeneously with a sample-to-paraffin weight ratio of 4:16, and then the mixture was pressed into a toroidal shape with an inner diameter of 2.0 mm and an outer diameter of 7.0 mm.

3. Data analysis

The *R2* value reflects the graphitization and the number of structural defects and assumes value higher than 0.5 for poorly organized structure and lower than 0.5 for a well-organized one, which can be calculated by the following formula (Eq. S1):

$$R2 = \frac{I_{D1}}{I_G + I_{D1} + I_{D2}} \qquad (Equation\ S1)$$

The band intensity ratio can be used to determine the degree of the graphitization, which can be calculated according to equation S2:

$$\frac{I_{D1}}{I_G} = C'(\lambda) d_{nc}^{-2} \qquad (Equation\ S2)$$

where C′ (514 nm) ≈ 0.0055 Å^{-2}.

The reflection loss (*RL*) values of the absorbers are calculated according to transmission line theory by the following equation S3-4:

$$R_L(dB) = 20lg\left|\frac{Z_{in} - Z_0}{Z_{in} + Z_0}\right| \qquad (Equation\ S3)$$

$$Z_{in} = Z_0 \sqrt{\frac{\mu_r}{\varepsilon_r}} \tanh\left[j\left(\frac{2\pi f d}{c}\right)\sqrt{\mu_r \varepsilon_r}\right] \quad (Equation\ S4)$$

Where Z_0 is the characteristic impedance of free space, Z_{in} is the normalized input impedance of absorber, ε_r and μ_r are the relative complex permittivity and permeability, d is the layer thickness, c is the speed of light in free space and f is the frequency.

$$SR_L = \frac{RL_{min}}{Thickness \times Loading} \quad (Equation\ S5)$$

Debye relaxation correction formula (Equation S6-7):

$$\varepsilon_r = \varepsilon_{r\infty} + \frac{\varepsilon_{rs} - \varepsilon_{r\infty}}{1 + (i\omega\tau)^{1-A}} \ (0 < A < 1) \quad (Equation\ S6)$$

$$\varepsilon_r^{'} = \varepsilon_{r\infty} + (\varepsilon_{rs} - \varepsilon_{r\infty})\frac{1 + (\omega\tau)^{(1-A)} sin\frac{\pi A}{2}}{1 + 2(\omega\tau)^{1-A} sin\frac{\pi A}{2} + (\omega\tau)^{2(1-A)}} \quad (Equation\ S7)$$

It is generally recognized that the Cole-Cole semicircle can be explained by the relaxation process, and the relationship between ε′ and ε″ can be expressed as (Equation S8):

$$(\varepsilon^{'} - \frac{\varepsilon_s + \varepsilon_\infty}{2})^2 + (\varepsilon^{''})^2 = (\frac{\varepsilon_s - \varepsilon_\infty}{2})^2 \quad (Equation\ S8)$$

Each semicircle in the ε′–ε″ curve stands for a polarization relaxation process. respectively. The high number of semicircles means the strong dipole polarization process.

The ability of microwave absorbers to attenuate electromagnetic wave energy is determined by the attenuation constant (α), which can be calculated by the following formula (Eq. S9):

$$\alpha = \frac{\sqrt{2}\pi f}{C}\sqrt{(\mu^{''}\varepsilon^{''} - \mu^{'}\varepsilon^{'}) + \sqrt{(\mu^{''}\varepsilon^{''} - \mu^{'}\varepsilon^{'})^2 + (\mu^{'}\varepsilon^{''} + \mu^{''}\varepsilon^{'})^2}} \quad (Equation\ S9)$$

4. Results and discussions

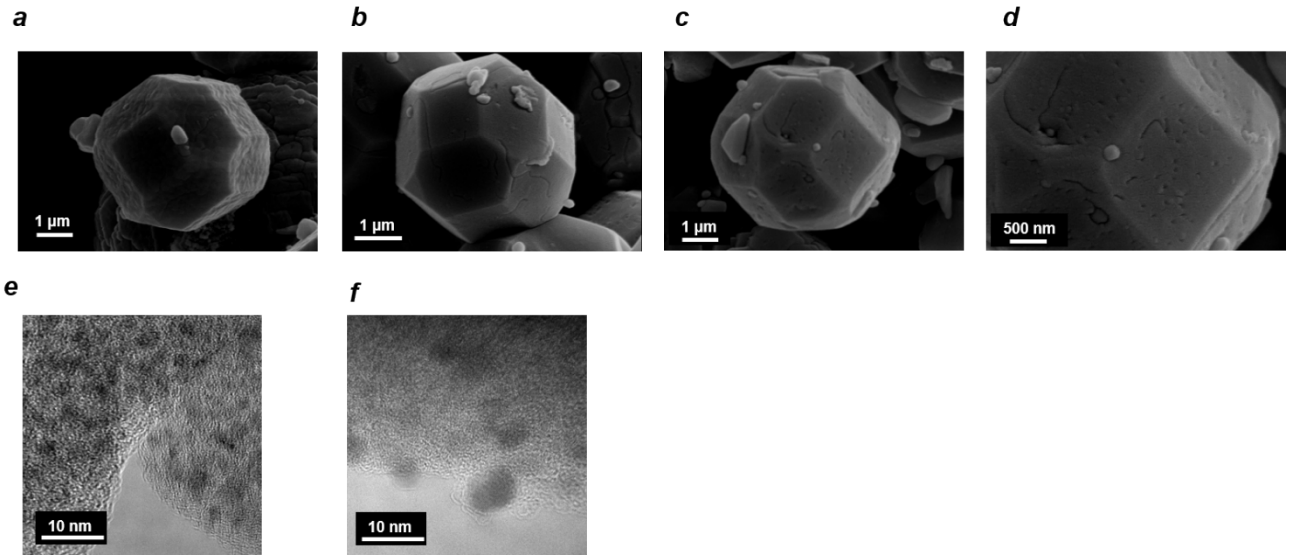

Figure S1 a-d, SEM images. **e-f,** TEM images of MoC

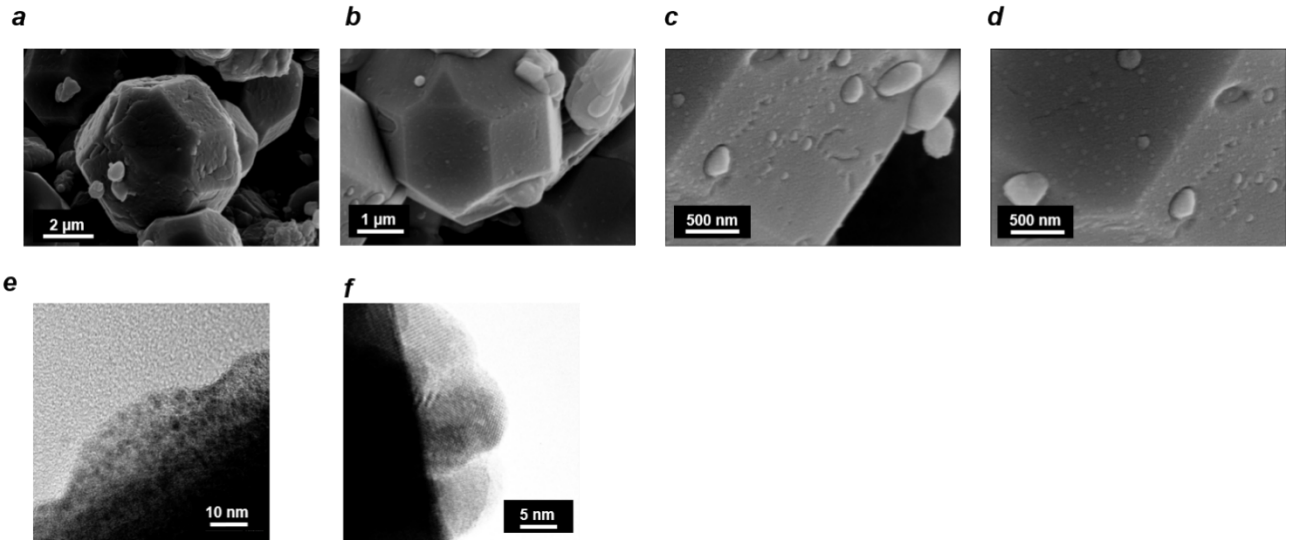

Figure S2 a-d, SEM images. **e-f,** TEM images of MoC@Ag-0.5

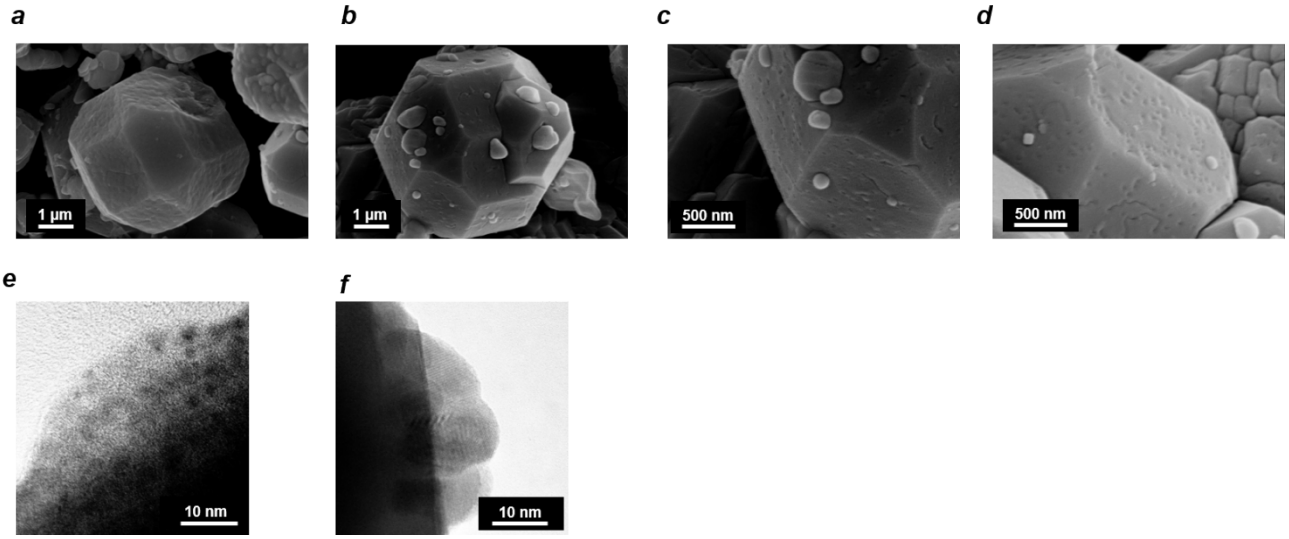

Figure S3 a-d, SEM images. **e-f,** TEM images of MoC@Ag-1.0

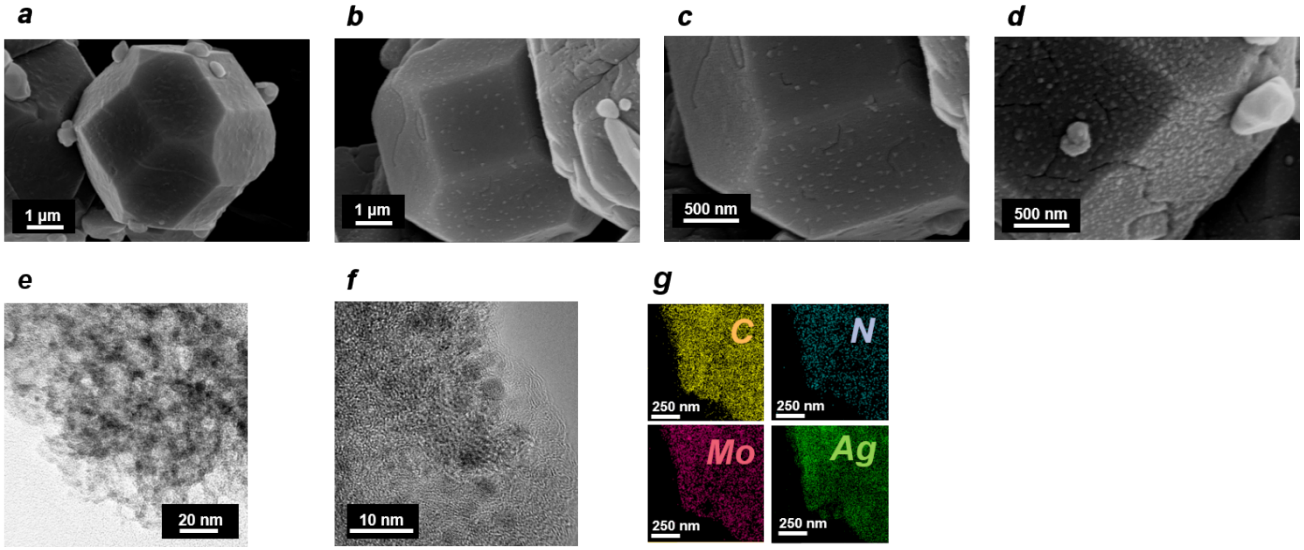

Figure S4 a-d, SEM images. **e-f,** TEM images.The elemental mapping images of C, N, Mo and Ag elements of MoC@Ag-1.5 .

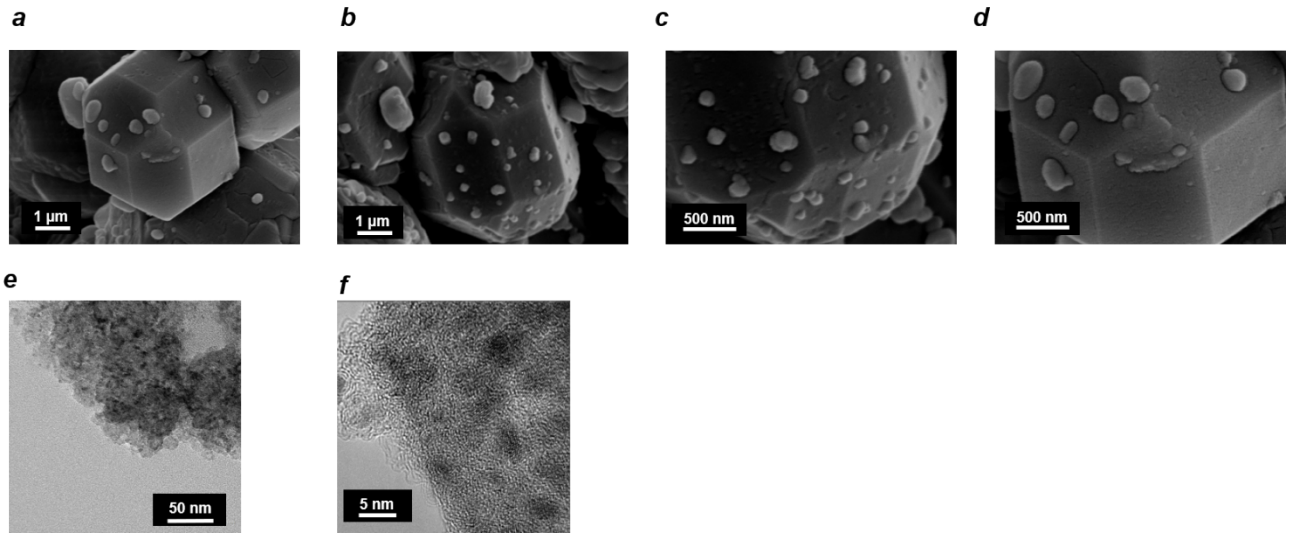

Figure S5 a-d, SEM images. **e-f,** TEM images of MoC@Ag-2.0

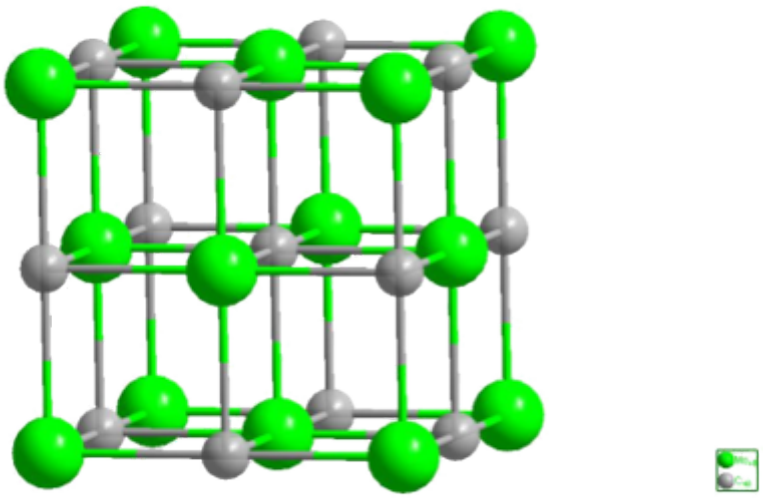

Figure S6 | The crystalline structures of (a) MoC

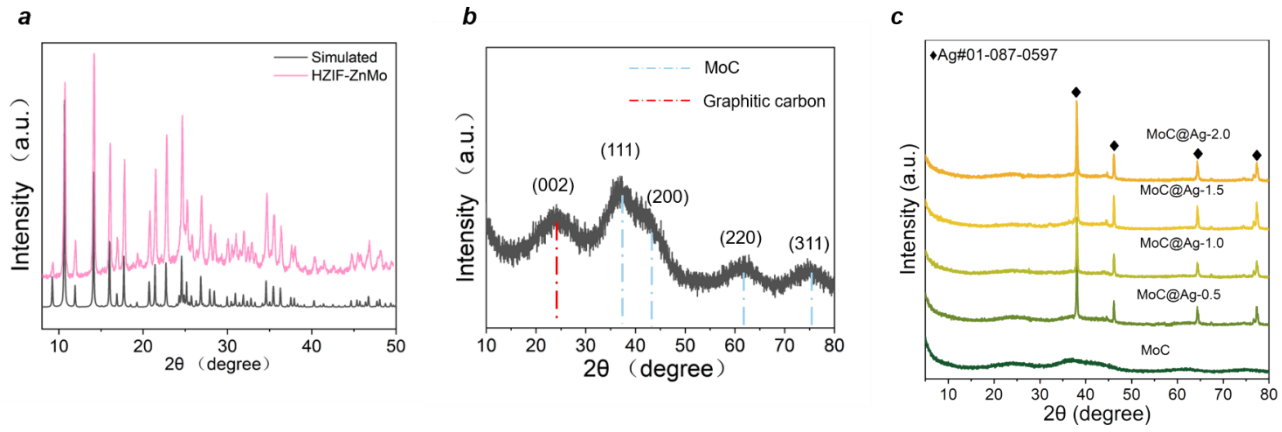

Figure S7 a,the XRD results of synthesized for HZIF-ZnMo, b-c MoC, MoC@Ag-0.5 h , MoC@Ag-1.0 h, MoC@Ag-1.5 h,and MoC@Ag-2.0 h

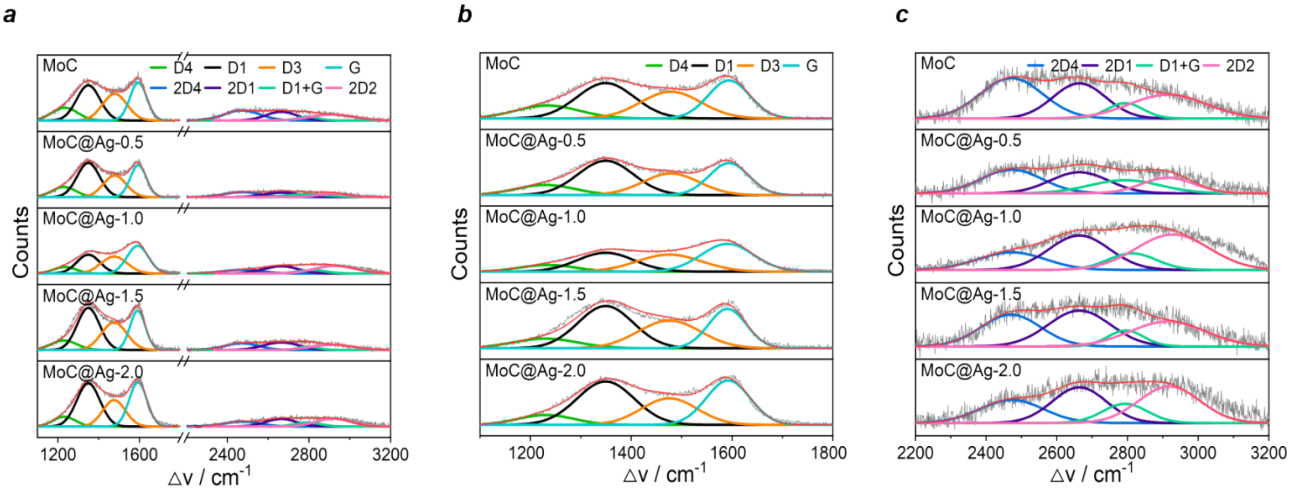

Figure S8.a, Full range Raman spectrum. **b-c,** Raman spectra deconvolution for MoC, MoC@Ag-0.5 h, MoC@Ag-1.0 h, MoC@Ag-1.5 h, and MoC@Ag-2.0h.

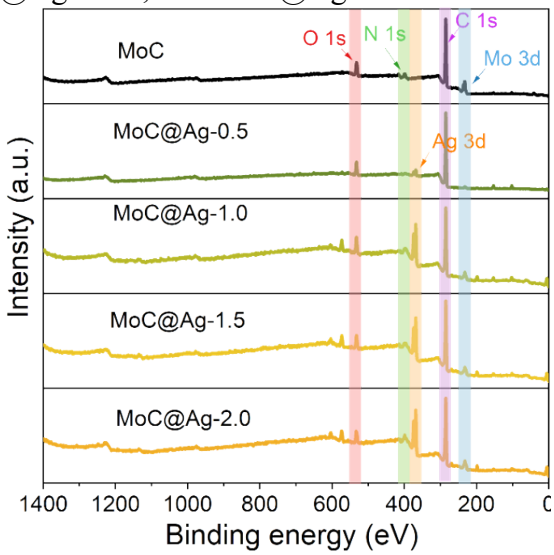

Figure S9. The survey XPS spectrum for MoC, MoC@Ag-0.5 h, MoC@Ag-1.0 h, MoC@Ag-1.5 h, and MoC@Ag-2.0 h

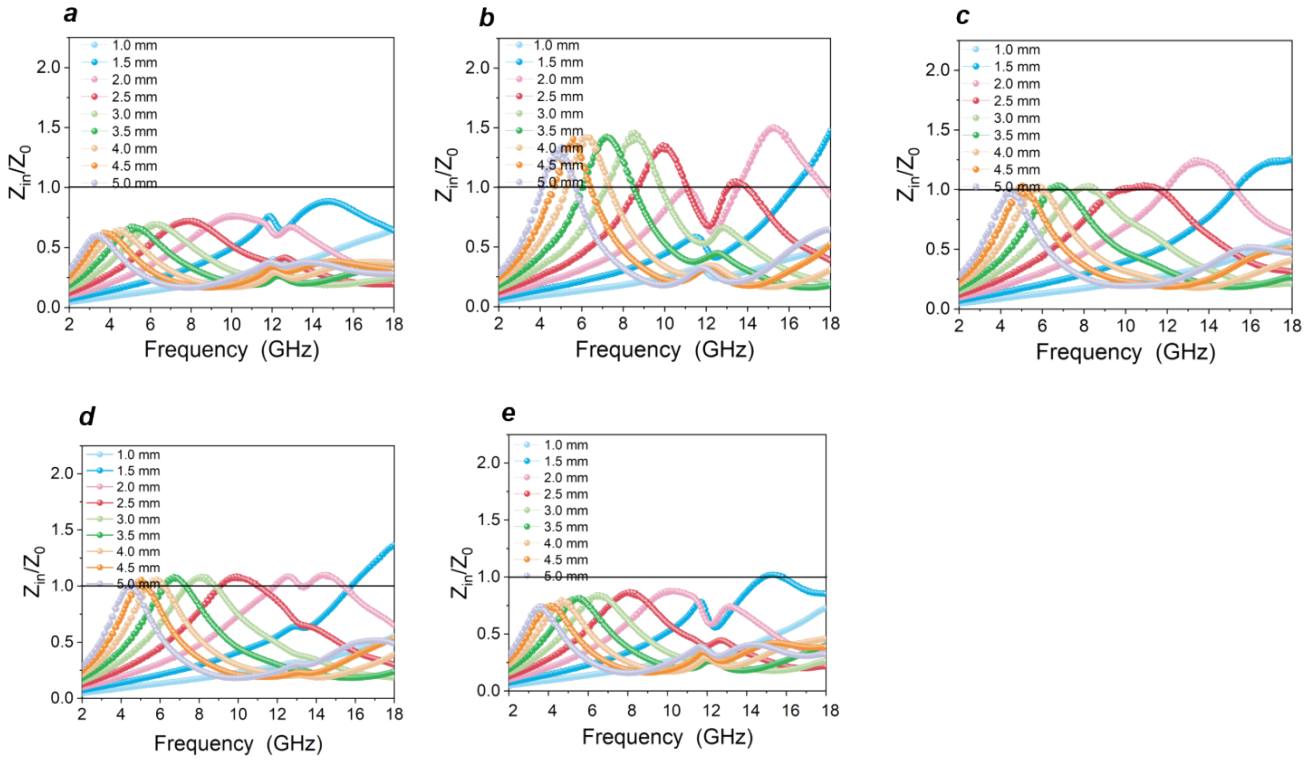

Figure S10. The $|Z_{in}/Z_0|$ plot of **a,** MoC, **b,** MoC@Ag-0.5 h, **c,** MoC@Ag-1.0 h, **d,** MoC@Ag-1.5 h, and **e,** MoC@Ag-2.0 h

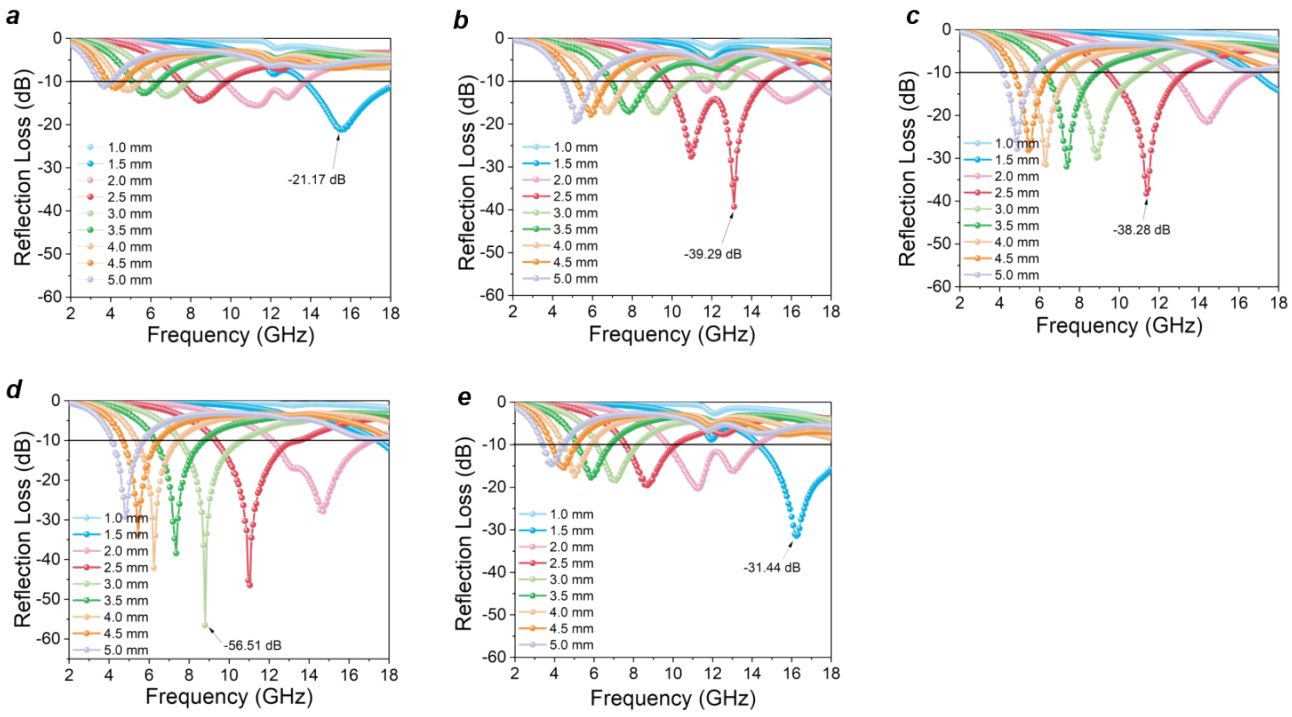

Figure S11. *RL* plots o **a,** MoC, **b,** MoC@Ag-0.5 h, **c,** MoC@Ag-1.0 h, **d,** MoC@Ag-1.5 h,and **e,** MoC@Ag-2.0 h

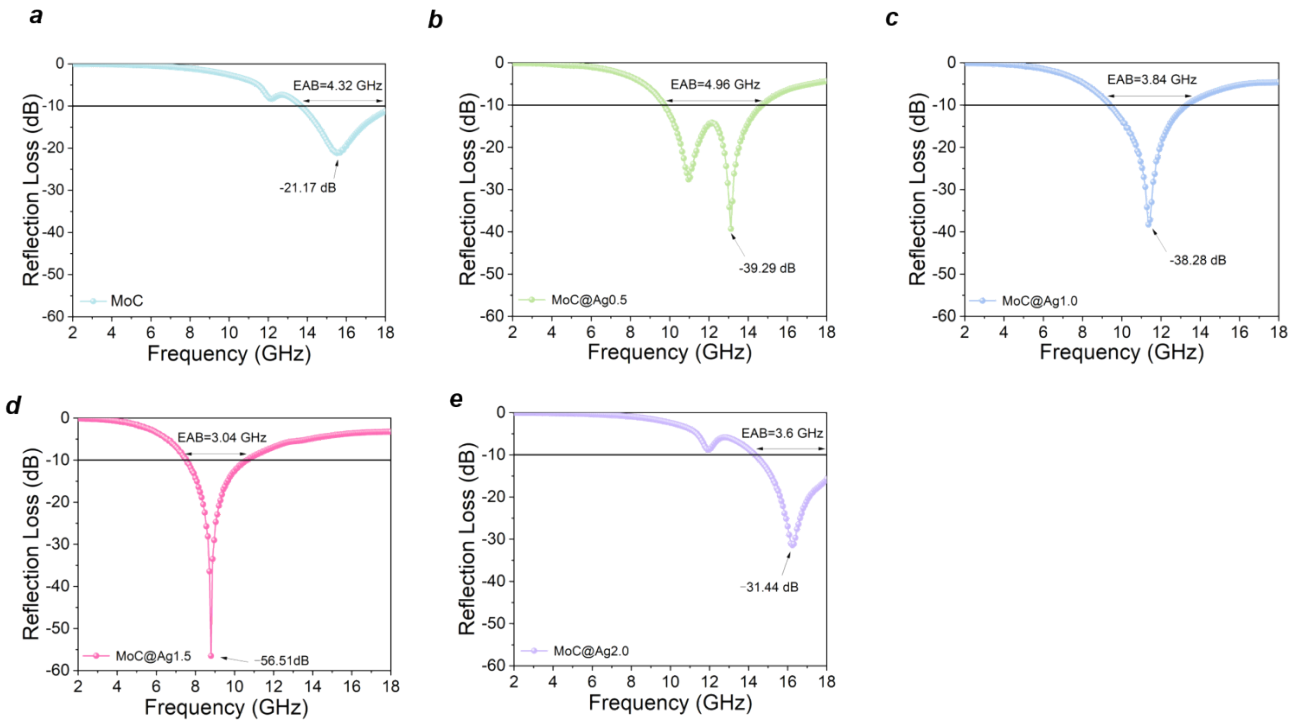

Figure S12. The effective absorbing band (<-10 dB) in RL plots of **a,** MoC, **b,** MoC@Ag-0.5 h, **c,** MoC@Ag-1.0 h, **d,** MoC@Ag-1.5 h, and **e,** MoC@Ag-2.0 h

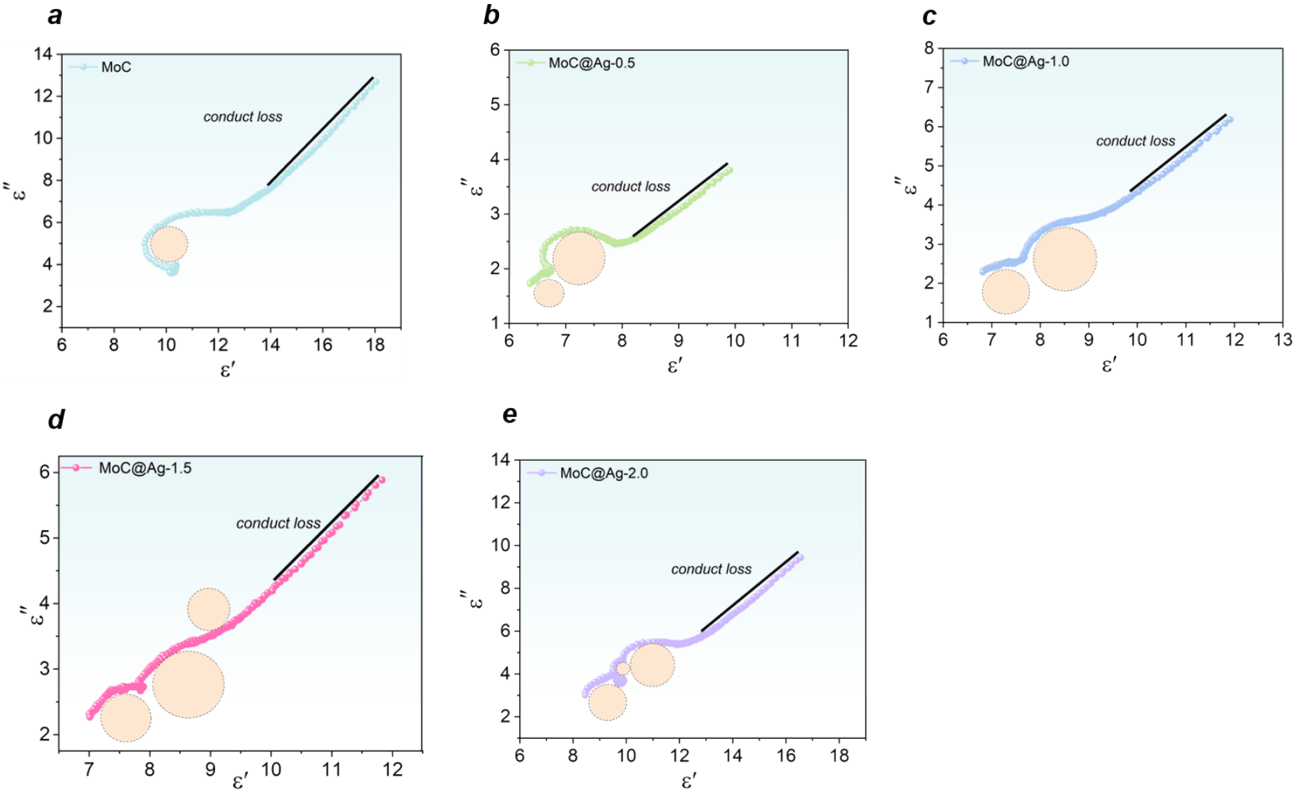

Figure S13. The *Cole-Cole* curves of **a,**MoC, **b,** MoC@Ag-0.5 h , **c,** MoC@Ag-1.0 h, **d,**MoC@Ag-1.5 h, and **e,** MoC@Ag-2.0 h

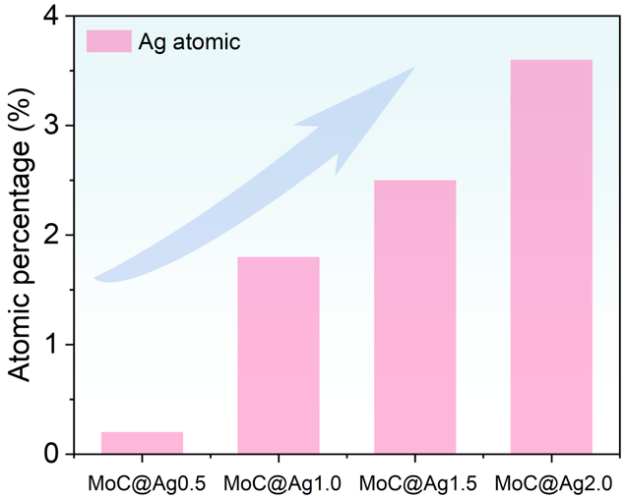

Figure S14. Elemental Ag content of samples of MoC@Ag-0.5 h, MoC@Ag-1.0 h, MoC@Ag-1.5 h and MoC@Ag-2.0 h.

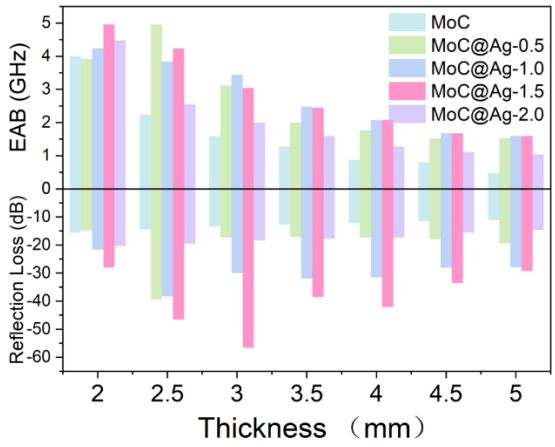

Figure S15 The EAB and RL_{min} values at different thickness of MoC, MoC@Ag-0.5 h , MoC@Ag-1.0 h,MoC@Ag-1.5 h,and MoC@Ag-2.0 h.

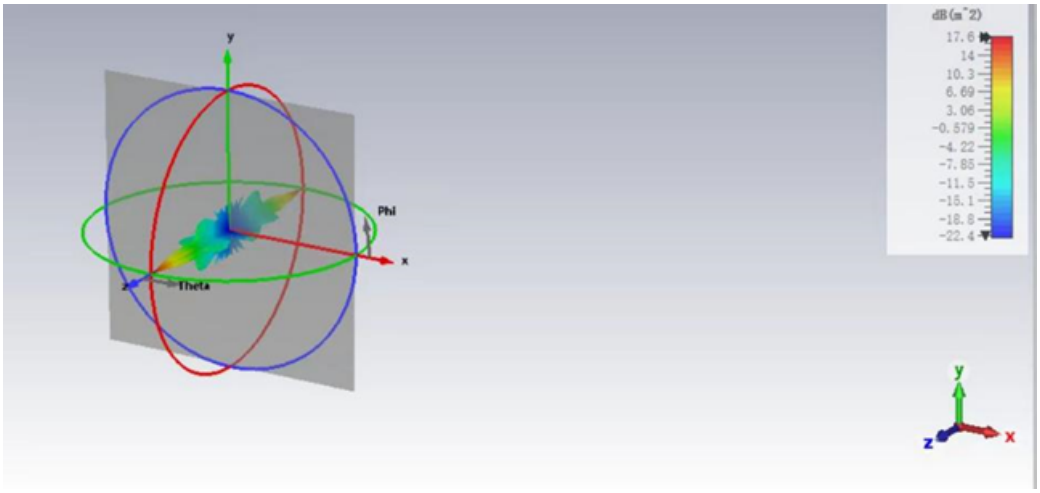

Figure S16 RCS simulation of a perfectly conductive layer（PEC）

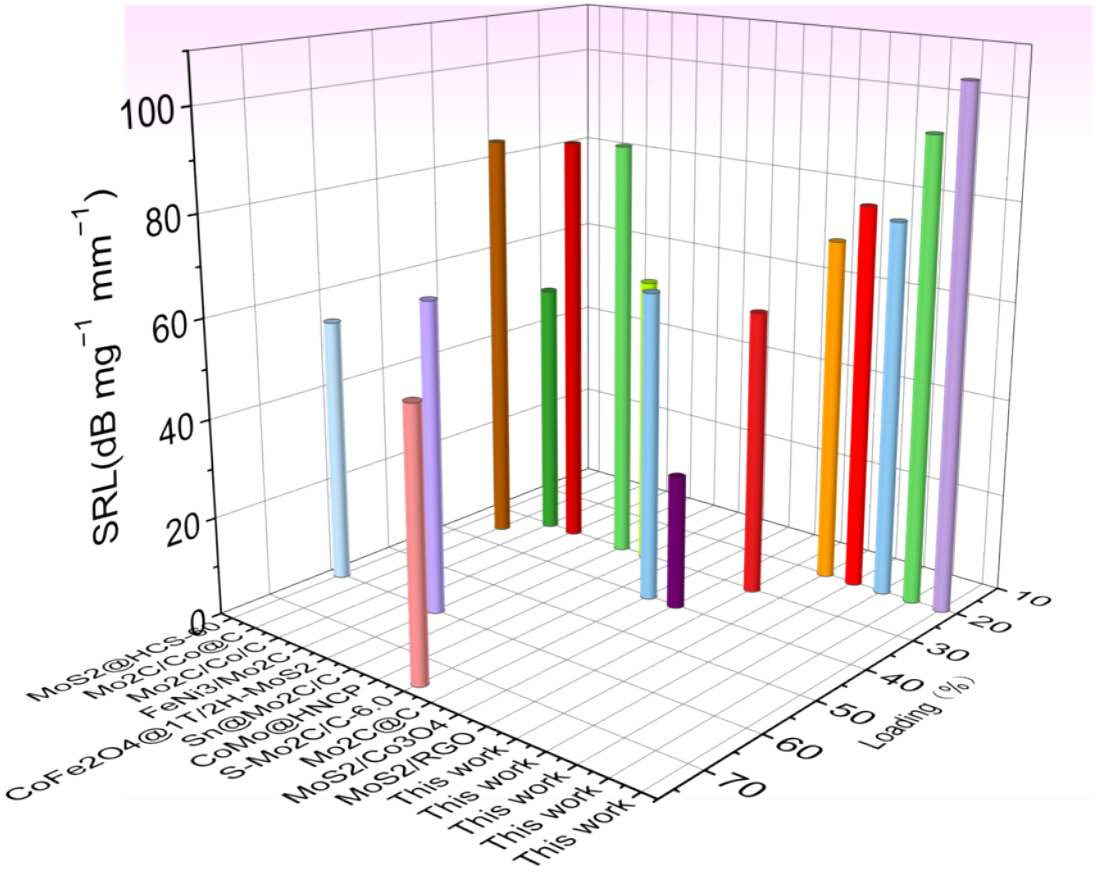

Figure S17 the comparison of *SRL* and Loading for MoC/Co@Ag with reported EWAMs in literatures.

Table S1. Raman parameters obtained from deconvolution spectra.

Sample	**Raman**											
	D1	G	A_{D3}	I_{D1}/I_G	R2	d_{nc}	2D4	2D1	A_{2D1}	D1+G	2D2	I_{2D1}/I_{D1}
	cm^{-1}	cm^{-1}				nm	cm^{-1}	cm^{-1}		cm^{-1}	cm^{-1}	
MoC	1349	1594	73.4	0.93	0.48	1.3	2472	2464	30.1	2793	2914	0.25
MoC@Ag-0.5	1349	1594	55.4	1.07	0.52	1.4	2472	2464	17.1	2793	2914	0.13
MoC@Ag-1.0	1349	1591	50.2	0.68	0.41	1.11	2472	2464	28.9	2812	2928	0.39

MoC@Ag-1.5	1349	1591	78.2	1.07	0.52	1.40	2470	2464	31.1	2795	2914	0.18
MoC@Ag-2.0	1349	1592	67.2	0.99	0.50	1.34	2472	2464	26.7	2793	2918	0.18

All Raman spectra were fitted with four bands. The frequency of the two bands corresponding to D1 and G were allowed to vary between 1300 and 1400 cm^{-1} and between 1550 and 1650 cm^{-1}, respectively. The frequency of the D3 band for amorphous carbon and D4 band tentatively assigned to polyenes or oligomers were fixed at 1500 cm^{-1} and 1200 cm^{-1}, respectively.

Table S2. Comparison of microwave absorption performance of α-MoC@Ag with other MOFs-derived carbon absorbers.

Samples	Thickness (mm)	Loading (wt%)	RL_{min} (dB)	SRL ($dB \cdot mg^{-1} \cdot mm^{-1}$)	Ref.
MoS_2@HCS-60 wt %	2.0	60	-65.00	-54.16	[1]
Mo_2C/Co@C nanorods	1.6	35	-47.98	-85.68	[2]
Mo_2C/Co/C	3.0	30	-48.00	-53.33	[3]
$FeNi_3/Mo_2C$	2.0	30	-51.5	-85.83	[4]
$CoFe_2O_4$@1T/2H-MoS_2	1.8	60	-68.50	−63.42	[5]
Sn@Mo_2C/C	2.0	30	-52.1	-86.83	[6]
CoMo@HNCP	2.0	40	−44.8	−59.73	[7]
S-Mo_2C/C-6.0	1.5	75	-60.4	-53.69	[8]
Mo_2C@C nanospheres	1.9	40	−48	−63.15	[9]
MoS_2/Co_3O_4	4	40	−43.56	−27.225	[10]
MoS_2/RGO	2.4	30	−41.9	−58.19	[11]
MoC@NC	1.5	20	−21.17	−70.59	this work

α -MoC@Ag-0.5	2.5	20	−39. 29	−78. 59	this work
α -MoC@Ag-1.0	2.5	20	−38. 28	−76. 56	this work
α -MoC@Ag-1.5	3.0	20	−56. 51	−94. 18	this work
α -MoC@Ag-2.0	1.5	20	−31. 44	−104. 80	this work

5. References

1. M. Ning, Q. Man, G. Tan, Z. Lei, J. Li and R.-W. Li, *ACS Applied Nano Mater*, 2020, **12**, 20785-20796.
2. Y. Wang, X. Li, X. Han, P. Xu, L. Cui, H. Zhao, D. Liu, F. Wang and Y. Du, *Chem Eng J*, 2020, **387**.
3. S. Dai, B. Quan, B. Zhang, X. Liang and G. Ji, *Dalton Trans*, 2018, **47**, 14767-14773.
4. C. Wu, K. Bi and M. Yan, *J. Mater. Chem. C*, 2020, **8**, 10204-10212.
5. X. Wang, T. Zhu, S. Chang, Y. Lu, W. Mi and W. Wang, *ACS Applied Nano Mater*, 2020, **12**, 11252-11264.
6. X. Qian, Y. Zhang, Z. Wu, R. Zhang, X. Li, M. Wang and R. Che, *Small*, 2021, **17**.
7. W. Huang, X. Zhang, Y. Zhao, J. Zhang and P. Liu, *Carbon*, 2020, **167**, 19-30.
8. Y. Wang, C. Li, X. Han, D. Liu, H. Zhao, Z. Li, P. Xu and Y. Du, *ACS Applied Nano Materials*, 2018, **1**, 5366-5376.
9. Y. Wang, X. Han, P. Xu, D. Liu, L. Cui, H. Zhao and Y. Du, *Chem Eng J*,, 2019, **372**, 312-320.
10. J. Chai, J. Cheng, D. Zhang, Y. Xiong, X. Yang, X. Ba, S. Ullah, G. Zheng, M. Yan and M. Cao, *J Alloys Compd*, 2020, **829**.
11. X. Wang, W. Zhang, X. Ji, B. Zhang, M. Yu, W. Zhang and J. Liu, *RSC Adv*, 2016, **6**, 106187-106193.